Dynamic hygrothermal behavior and energy performance analysis of a novel multilayer building envelope based on PCM and hemp concrete

Dongxia Wu, Mourad Rahim, Mohammed El Ganaoui, Rachid Bennacer, Rabah Djedjig, Bin Liu

Dynamic hygrothermal behavior and energy performance analysis of a novel multilayer building envelope based on PCM and hemp concrete

Dongxia Wu[a]; Mourad Rahim[a]; Mohammed El Ganaoui [a, *]; Rachid Bennacer[b]; Rabah Djedjig[a]; Bin Liu[c]

a. University of Lorraine, LERMAB, IUT H Poincaré de Longwy, 168 Rue de Lorraine. Cosnes et Romain, 54400 Longwy, France

b. University of Paris-Saclay, ENS Paris-Saclay, CNRS, LMT -, 91190, Gif-sur-Yvette, France

c. Tianjin Key Laboratory of Refrigeration Technology, Tianjin University of Commerce, Tianjin 300134, China

* Corresponding author. Tel: +33-0664947141; E-mail: mohammed.el-ganaoui@univ-lorraine.fr

Address: IUT Henri Poincaré de Longwy. 168 Rue de Lorraine. Cosnes et Romain, 54400 Longwy, France

Abstract

Phase change materials (PCMs) have high thermal inertia while hygroscopic materials have high hygric inertia. However, few studies have integrated the two materials and considered both hygrothermal behavior and energy performance. This study proposed a novel multilayer building envelope integrated by PCM and bio-based hygroscopic material (hemp concrete) to utilize the advantages of both materials. Four envelope configurations were experimental studied based on the presence and location of the PCM to study the effect of PCM and its location on the hygrothermal behavior and the energy performance of the integrated envelope. The results demonstrated the benefits

of PCM in reducing the temperature/relative humidity (T/RH) amplitude and energy consumption as well as delaying the peak T of the envelope. Placement of the PCM in the middle of the envelope was recommended, with the PCM kept in a partially melted state. Compared to the configuration without PCM, the T/RH amplitude and energy consumption were reduced by 50%/60% and 15.3%, respectively, and the peak T was delayed by 70.4%. The PCM placed on the outdoor side had the highest efficiency and energy participation, but it absorbed the most heat and was prone to overmelting. The envelope with PCM placed on the indoor side lost the benefit of regulating RH. This study provides a reference for multilayer envelopes composed of PCMs and hygroscopic materials and dedicated to T/RH regulation.

Keywords

Building envelope; Phase change material (PCM); Bio-based hygroscopic material; Hygrothermal behavior; Energy saving

1. Introduction

It is reported that building envelopes account for almost 50% of building energy consumption [1]. Therefore, research on building envelopes helps save energy and reduce CO_2 emissions in the context of the global energy crisis and global warming [2]. Meanwhile, designers strive to achieve indoor hygrothermal comfort, which is mainly assessed by temperature (T) and relative humidity (RH) [3]. Improper combinations of T and RH may adversely affect the occupants' health [4, 5] and increase the

risk of indoor mold growth [6, 7]. Therefore, the related characteristics of the building envelope are important for energy saving, environmental protection, and indoor comfort.

Bio-based materials are generally made from biologically renewable materials such as wood, hemp, straw, etc. [8, 9]. These materials have received a lot of attention in recent years thanks to their advantages. The renewable nature and low carbon emissions characteristic of bio-based materials are significant. They have a low carbon emission during manufacturing, installation, utilization, maintenance, and demolition [10, 11]. Some bio-based materials also have high porosity and low thermal conductivity, making them useful insulation materials for building envelopes. Liu et al. [12] reviewed the development history of bio-based materials as building insulation, and listed the four most popular bio-based materials: hemp, straw, flax, and wood. Moreover, the hygroscopic properties of bio-based materials can regulate the amount of water vapor in the air to maintain the RH balance [13, 14], which is attributed to their porous structure. The hygroscopic properties have been proven to affect energy consumption and HVAC (heating, ventilation, and air conditioning) system design. For buildings with hygroscopic envelopes, the HVAC structure can be reduced by 13% [15], while cooling energy consumption can be reduced by 5–30% [16].

The hygrothermal properties of bio-based materials have been studied by many researchers hoping to integrate them into the building envelope. In a typical laboratory study of a given envelope, the materials were usually placed between a controlled climate chamber and the laboratory environment, or directly between two controlled climate chambers. Colinart et al. [17] compared the hygrothermal behavior of uncoated and coated hemp concrete walls by placing them between two climatic chambers. The results showed that the vapor pressure gradient was the main driving potential,

and that coatings could dampen heat and moisture transfer through the hemp concrete. Chennouf et al. [18] imitated indoor and outdoor environments using a passive shell and a climate chamber to study the hygrothermal behavior of date palm fiber concrete. The hygrothermal response showed the potential of utilizing the hygric inertia. Furthermore, the T dependence of hygric behavior has been noted and investigated [19, 20]. Rahim et al. [21] investigated the hygrothermal behavior of hemp and straw rape concrete, and found that the impact of T on RH within the material was more significant than the water vapor pressure gradient. They emphasized the importance of the T effect on sorption curves. Poyet et al. [22] proposed the theoretical background of the Clausius-Clapeyron equation and the isosteric heat of sorption to describe the impact of T on the sorption properties. This theory was confirmed by Colinart et al. [23, 24], who studied the RH variations in three bio-based materials. To sum up, the bio-based materials have hygric inertia to dampen the RH variation; it is significantly affected by T.

Integrating phase change materials (PCMs) into the building envelope is another promising technique. PCMs can store and release large amounts of latent heat during the phase change process, which makes them have high thermal inertia [25, 26]. As a building envelope, they can be used in different seasons, countries, and climates [27] to manage the thermal environment, improve the occupants' comfort, and save energy [28-30].

Consequently, bio-based hygroscopic materials have the advantage of hygroscopic properties, but their low density and low heat capacity make them low thermal inertia. On the other hand, PCMs have a large capacity for thermal energy storage and release, but they can only regulate thermal behavior but not hygric behavior. In previous research, the advantages of these two materials have always been

studied separately. Therefore, it would be meaningful and innovative to integrate the two types of materials and utilize their respective advantages. In this study, a common approach of envelope assembly, i.e., multilayer assembly, was used to integrate the two types of materials.

Multilayer integrating PCMs with porous materials such as gypsum [31], plaster [32], wood[33], and concrete [34] are the most widespread approach for latent heat energy storage in building elements. The location of PCM in the multilayer envelope has been proven to affect the thermal behavior of the envelope. Lee et al. [35] assessed a south and west wall by integrating a PCM at different locations, and found that the optimum location depended on the wall's orientation. Fateh et al. [36, 37] used a simulation method to study the thermal performance of a light wall with PCMs placed at different locations, and the optimum location in their test conditions was the middle. Likewise, Kishore et al. [38, 39] studied the optimum location in five U.S. cities, and the optimum location of PCMs was the middle of the envelope. Murathan et al. [40] evaluated the energy consumption when placing a PCM in different locations, and found that the envelope with the PCM placed between the middle and the outside consumes less energy. Li et al. [41] investigated the optimum PCM location by evaluating the heat flux, and the highest heat flux reduction was 47.6% when the PCM was placed close to the exterior. However, these studies mainly focused on thermal behavior and energy performance while ignoring hygric behavior, even though the porous materials (gypsum, plaster, wood, and concrete) that are part of the PCM multilayer envelope have been shown to have hygroscopic properties [42-45]. Moreover, considering the T-dependent hygric behavior of hygroscopic material and the location-dependent thermal behavior of PCM, it can be inferred that the PCM location affects the hygric behavior of the envelope. However, this inference has not been studied or proven in the

104 previous literature. Therefore, it is necessary to explore the effect of PCM and its location on the
105 thermal and hygric behavior as well as the energy performance of the integrated envelope.
106 Furthermore, since buildings are constantly exposed to climatic variations, continuous dynamic
107 boundary conditions should be considered for several days to access the hygrothermal dynamic of the
108 envelope, not just transient from initial conditions to a partially state.

109 In this study, a novel multilayer building envelope integrated by bio-based hygroscopic material
110 and PCM was proposed to simultaneously regulate T and RH and save energy of buildings. The
111 bio-based hygroscopic material used in this paper was hemp concrete, whose hygroscopic properties
112 have been shown to be superior to conventional materials such as gypsum, plaster, and common
113 concrete [46]. The thermal and hygric behavior as well as energy performance of the integrated
114 envelope were experimentally investigated under imitated dynamic outdoor conditions. Three
115 envelope configurations with PCM placed in different locations were proposed and compared with the
116 configuration without PCM to study the effect of PCM and its location on hygrothermal behavior and
117 energy performance. Special attention was paid to the T/RH amplitude and time delay, especially in
118 the case where the location within the envelope was close to the interior. The energy performance of
119 the whole envelope and of the PCM layer was studied, the activation and energy storage/release
120 efficiency of the PCM in different locations were analyzed.

121

2. Materials and methods

2.1. Materials and their properties

The PCM panel [47] shown in Fig. 1(a, b) is a shape-stabilized PCM wrapped on both sides in an aluminum sheet with a thickness of 0.1 mm, preventing deformation and leakage during use. The main element producing the phase change is a mixture of 60% paraffin wax and 40% ethylene-based polymer. Fig. 1(e) shows the specific heat capacity of the PCM. It remains in the liquid-solid coexistence state during the phase change range from 10 to 28 °C, making its latent heat deduced as 136.2 kJ/kg. The maximum specific heat capacity corresponds to a T of 22°C.

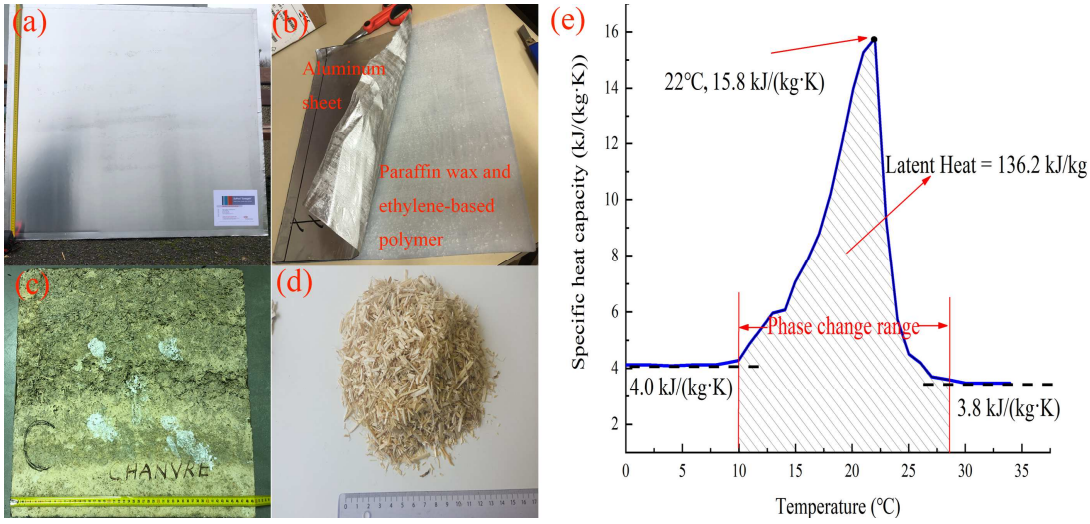

Fig. 1. (a) PCM panel; (b) Aluminum sheet and the mixture of paraffin wax and ethylene-based polymer; (c) Hemp concrete; (d) Hemp shives; (e) Specific heat capacity of the PCM [47]

The bio-based material used in this study is hemp concrete (Fig. 1(c)). It was composed of water (24%), a lime-based binder (12%), and hemp shives (64%, (Fig. 1(d))). Table 1 lists the dimensions

and basic hygrothermal properties of the PCM and the hemp concrete.

	PCM [47]	Hemp concrete [48]
Dimensions (L × W) (cm)	50 × 50	50 × 50
Thickness (cm)	2.12	7
Density (kg/m^3)	810	478
Thermal conductivity (W/(m·K))	Solid: 0.18; Liquid: 0.14	0.12
Specific heat capacity (kJ/(kg·K))	Solid: 4.0; Liquid: 3.8	1.08
Porosity (%)		76.44
Water vapor permeability (kg/(m·s·Pa))		2.23×10^{-11}

Table 1. Dimensions and hygrothermal properties of the PCM and the hemp concrete

2.2. Experimental facilities

To set the boundary conditions, a climate chamber (LabEvent L C/64/40/3) was used. It runs with an accuracy of ±0.3–1 °C in a T range of −40 to 180 °C and ±1–3% in an RH range of 10 to 95%. After the parameters are set, continuous humidification/dehumidification and heating/cooling take place automatically.

The sensors for measuring T and RH were thermocouples (K type) and HMP-110 sensors. The diameter of the thermocouples was 0.25 mm; they could measure a T range from −70 to 200 °C with an accuracy of ±0.1 °C. The HMP-110 sensors had an elongated cylindrical shape with a length of 71 mm

149 and a diameter of 12 mm. They were inserted into the hemp concrete layer from the lateral side to
150 measure the T and RH simultaneously, and the measurement ranges of T and RH were from –40 to 80 ℃
151 and from 0 to 100% with an accuracy of ±0.2 ℃ (0–40 ℃) and ±1.5% (0–90%), respectively. The heat
152 flux was monitored with HFS sensors with dimensions of 50 mm × 50 mm × 0.5 mm; the measurement
153 range was –2.0 to 2.0 kW/m^2 with an accuracy of ±2%.
154 The data acquisition system (Keithley 2700, with a resolution of 6.5 digits) was connected to a
155 computer. All the data were collected and recorded automatically with time intervals of 120 seconds.
156

157 **2.3. Methodology**

158 The overview schematic of the experiment is shown in Fig. 2(a). One side of the envelope was
159 connected to a climate chamber to imitate the outdoor environment. The other side of the envelope was
160 exposed to the laboratory environment with a relatively stable hygrothermal environment to imitate the
161 indoor environment of a real building. Fig. 2(b) shows the actual experimental setup. To ensure
162 thermal and moisture insulation in the transversal plan (perpendicular to the thickness), polystyrene
163 foam and polyethylene film were wrapped around the lateral envelope sides.
164 The envelope elements consisted of one PCM layer and two hemp concrete layers. To explore the
165 effect of PCM and its location on the hygrothermal behavior and the energy performance of the
166 envelope, three integrated envelope configurations (X = 0 L, X = 0.5 L, and X = 1 L) with PCM placed
167 in different locations were proposed to compare with a configuration without PCM. They were given
168 the following names and descriptions (Fig. 2(c)):

1. Configuration without PCM: Two hemp concrete layers without PCM;
2. Configuration X = 0 L: PCM was placed on the outdoor side (climate chamber), and L denotes the total thickness of the two hemp concrete layers;
3. Configuration X = 0.5 L: PCM was placed between the two hemp concrete layers;
4. Configuration X = 1 L: PCM was placed on the indoor side (laboratory environment).

It should be noted that the transferability of heat/moisture or the accuracy of results were not affected when two hemp concrete layers are in direct contact (configuration without PCM, X = 0 L, and X = 1 L), because the T and RH were constant on the interface of the two hemp concretes [49-51].

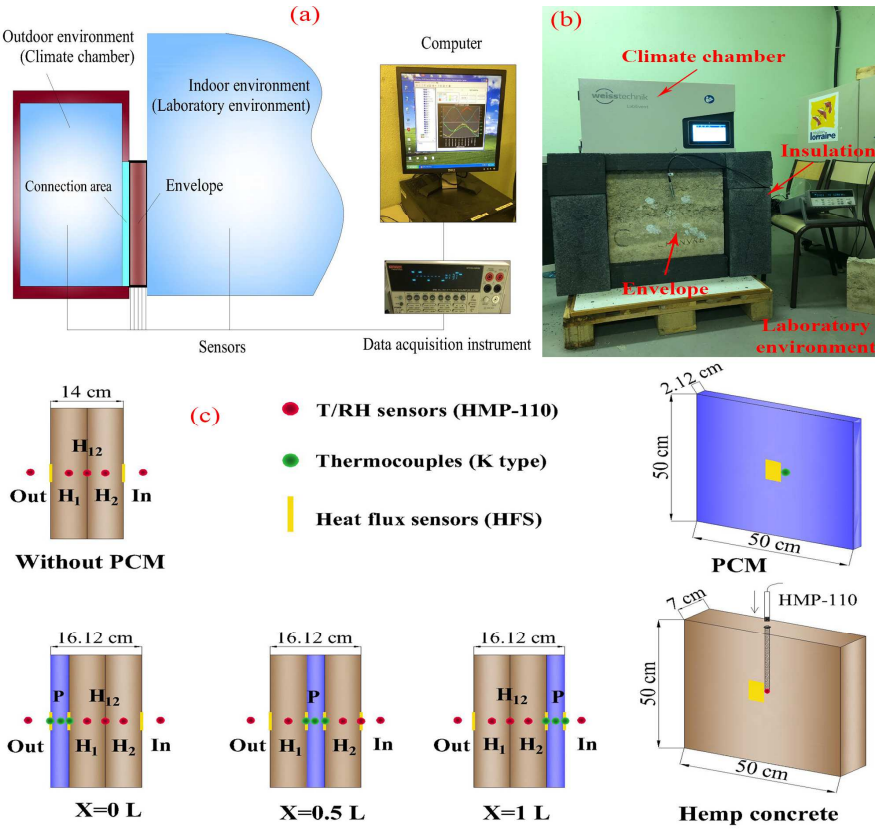

Fig. 2. (a) Diagram of the experimental setup; (b) Actual experimental setup; (c) Four envelope configurations

The main measurement points are also shown in Fig. 2(c), their names are given below:

- Out: outdoor environment (climate chamber)
- In: indoor environment (laboratory environment)
- H_1: middle of the first hemp concrete layer
- H_{12}: between the two hemp concrete layers
- H_2: middle of the second hemp concrete layer
- P: middle of the PCM layer

Furthermore, some heat flux sensors were affixed on each side of the PCM and the whole envelope.

Fig. 3 shows the fluctuations of T and RH provided by the climate chamber (outdoor). Due to the large phase change range of the PCM as shown in Fig. 1(e), a large diurnal T range of 15 to 40 °C (e.g., summer climate of Ruoqiang, China) was chosen to better observe the T and RH fluctuations at different locations within the hemp concrete. The overall T range contains five smaller T ranges to represent various weather conditions: cool (15–20 ℃), temperate (20–25 ℃), warm (25–30 ℃), hot (30–35 ℃), and very hot (35–40 ℃) [52]. On the one hand, the large T range helps to observe the feedback of the envelope to cold T, very hot T, and the T between them. On the other hand, if the integrated envelope is shown to be applicable over a large T range, it is also applicable over a small T range. The RH was set to a range of 25% to 95%, which represented the variation centered on a comfortable level (60%) and fluctuating between extremely dry (25%) and humid (95%) conditions. The combination of T and RH represented dynamic boundary conditions in the outdoor environment

with a wide T/RH range but little vapor pressure fluctuations. In the beginning, the T and RH were held at 27.5 ℃ and 70% for two days until stabilization. Then the T and RH evolved periodically for seven days according to the sinusoidal function with time (day) as the variable:

$$T = 27.5 + 12.5sin\left(\frac{\pi}{12}t\right)$$

$$RH = 60 - 35sin\left(\frac{\pi}{12}t\right)$$

As for the hygrothermal conditions in the laboratory environment (indoor), they were relatively stable during the experiment, with a T of 21.4 ± 0.7 ℃ and RH of 45.2 ± 5.1%. Thus, one side of the envelope was exposed to a dynamic condition, while the other side faced a relatively stable condition.

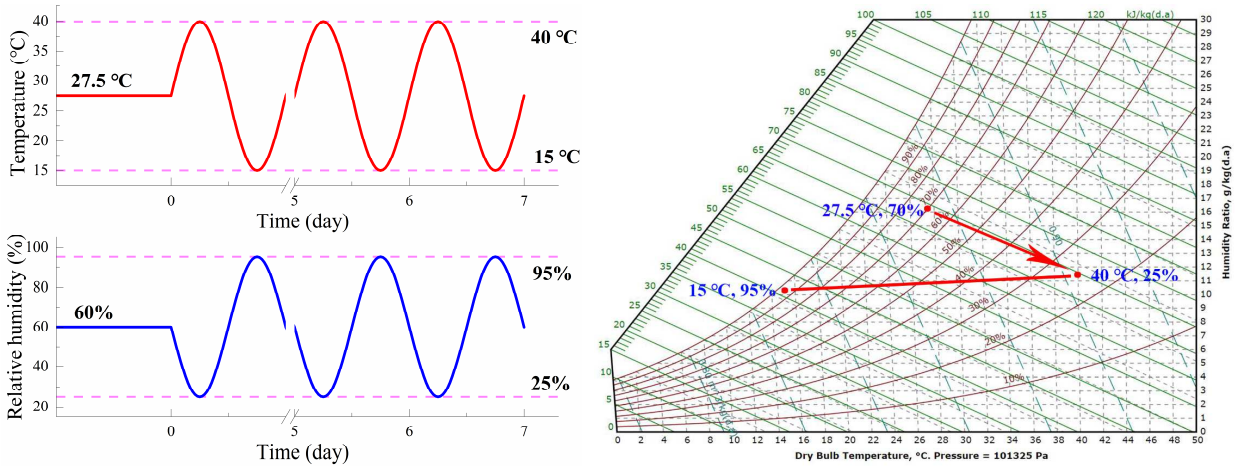

Fig. 3. Imposed oscillating outdoor boundary conditions

3. Results and discussion

3.1. Hygrothermal behavior of the configuration without PCM

Fig. 4 represents the hygrothermal behavior of the configuration without PCM, which had unrestricted transfer of heat and moisture on each side of the envelope. For the boundary conditions,

the T_{out} and RH_{out} (T and RH in the outdoor environment, i.e., in the climate chamber) evolved well and matched the set values. In the laboratory environment, the T and RH remained relatively stable. The T_{hemp} and RH_{hemp} (T and RH within the hemp concrete, i.e., at H_1, H_{12}, and H_2) kept a steady state 4 h (0.17 days) before the start of the dynamic change, and their respective standard deviations were below 0.03 °C and 0.05%, respectively.

T_{hemp} was mainly affected by the T_{out}. The T amplitudes at points H_1, H_{12}, and H_2 decreased sequentially, with values of 6.1, 4.2, and 2.4 °C, respectively. There was a response time delay between the outdoor environment and the envelope, with average time delays of 2.1, 3.0, and 3.7 h at points H_1, H_{12}, and H_2, respectively.

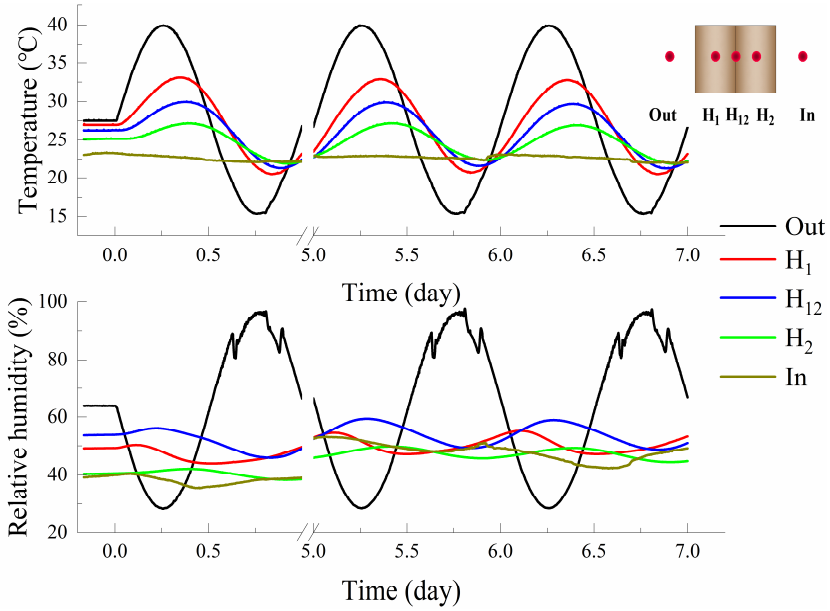

Fig. 4. Hygrothermal behavior of the configuration without PCM

Compared to the T_{hemp}, the RH_{hemp} variation was more complex, which can be inferred from the RH_{hemp} at H_1 and H_{12}. Both the overall value (45.5–52.7%) and the amplitude (3.6%) of RH_{hemp} at H_1

were lower than those at H_{12} (48–58.1% and 5.1%). These phenomena were caused by the superposition effect within the hemp concrete.

Before explanation, the two effects caused by boundary conditions T and RH were introduced. In previous similar studies, the boundary T/RH of the envelope was set almost as static or from one static to another [17-20]. Few studies [21] have covered the dynamic boundary T/RH. Generally, the effect of one parameter (T or RH) on the RH variation within the materials can be analyzed under static-to-static boundary conditions while keeping the other parameter constant. Using this method, Chennouf et al. [18] and Colinart et al. [17] investigated the effect of boundary RH and T on the RH variation within the material, respectively.

Specifically, in this study, the increase of T_{out} led to the instantaneous moisture evaporation within the hemp concrete, which led to the increase of the RH_{hemp}. Conversely, the decrease in T_{out} led to moisture condensation and a decrease in the RH_{hemp}. On the other hand, the increase in RH_{out} led to moisture diffusion from the outdoors to the envelope, and therefore increased the RH_{hemp}. Conversely, the decrease in RH_{out} caused the evacuation of the vapor out of the hemp concrete and decreased the RH_{hemp}. Thus, the dynamically opposite variations of boundary T_{out} and RH_{out} had opposite transient effects on RH_{hemp} variation. As for different points, the effect of RH_{out} was strong at points close to the outdoors (H_1) but weak at points far away from the outdoors (H_{12} and H_2), which can be inferred from two aspects. First, the overall values and amplitudes of RH_{hemp} at H_1 were smaller than that of H_{12}. Because the decreased/increased RH_{out} inhibited the increase/decrease of RH_{hemp} caused by the increased/decreased T_{out}. Second, the time difference between peak/valley RH_{hemp} and peak/valley T_{hemp} was longer at point H_1 than that of point H_{12} and H_2, and the longer time difference implied

254 stronger competition between the effects of RH_{out} and T_{out}. At point H_1, the peak RH_{hemp} appeared 6.3
255 h earlier than the peak T_{hemp}. In contrast, at points H_{12} and H_2, the corresponding values were 1.9 and
256 0.03 h, respectively. Therefore, RH_{hemp} variations at point H_1 were affected by the superposition effect
257 of T and RH, while at point H_{12} and especially H_2, RH_{hemp} variations were mainly affected by T.
258 Rahim et al. [21] have reported similar T_{hemp}/RH_{hemp} variation in the middle of the envelope and
259 close to the outdoors (corresponding to H_{12} and H_1 in this paper, respectively). However, the points
260 close to the indoor side (H_{12} and especially H_2) are the main interest to us, because their T/RH behavior
261 influences indoor hygrothermal comfort. Therefore, the T/RH behavior of H_{12} and H_2 will be the focus
262 of the following sections.
263
264 **3.2. Hygrothermal behavior of the configurations with PCM**
265 **3.2.1. PCM placed on the outdoor side (X = 0 L)**
266 Fig. 5 shows the hygrothermal behavior of the configuration X = 0 L. The standard deviations of T
267 and RH in hemp concrete and PCM were below 0.06 °C and 0.09% during 4 h preceding the start of the
268 dynamic change, indicating that the dynamic change started from a steady state. Importantly, the PCM
269 was impermeable to moisture, meaning that there was no moisture transfer from the outdoor side to the
270 envelope, but the moisture transfer between the envelope and the indoor environment was not affected.
271 As for heat transfer, it can occur through any material.
272 Regarding the T variation, the T amplitude was smaller and the time delay was longer than in the
273 configuration without PCM. At H_1, H_{12}, and H_2, the T amplitudes were reduced by 1.6, 1.2, and 0.4 °C,

and the time delays were extended by 2.4, 2.4, and 2.1 h, respectively, because PCM damped the heat transfer between the hemp concrete and the outdoor side.

For the RH, the amplitudes at H_{12} and H_2 were 2.9 and 1.9%, which was 2.2 and 0.1% less than in the configuration without PCM. As mentioned above, the RH at H_{12} and H_2 was mainly influenced by T variation, so their RH amplitudes decreased with the reduction of the T amplitude.

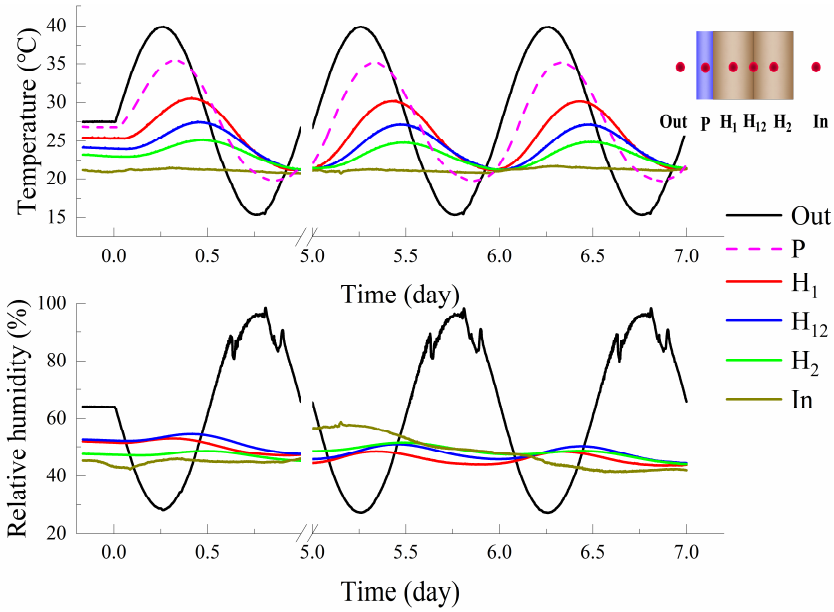

Fig. 5. Hygrothermal behavior of the configuration X = 0 L

3.2.2. PCM placed between two hemp concrete layers (X = 0.5 L)

The PCM was placed between the two hemp concrete layers in this configuration, and the heat/moisture transfer could occur on both sides of the envelope. In Fig. 6, the T amplitudes at H_1 and H_2 were 5.7 and 2.1 °C, respectively, both smaller than in the configuration without PCM. However, the amplitude at H_1 was reduced by only 6.5%, while at H_2 it was as high as 50%, because the PCM's

thermal inertia had a greater effect on H_2. Likewise, the time delay at H_2 was more noticeable, which is extended by 2.3 h compared to the configuration without PCM.

Due to the effect of T amplitude, the RH at H_2 was significantly reduced, from 2.0 to 0.8% compared to the configuration without PCM.

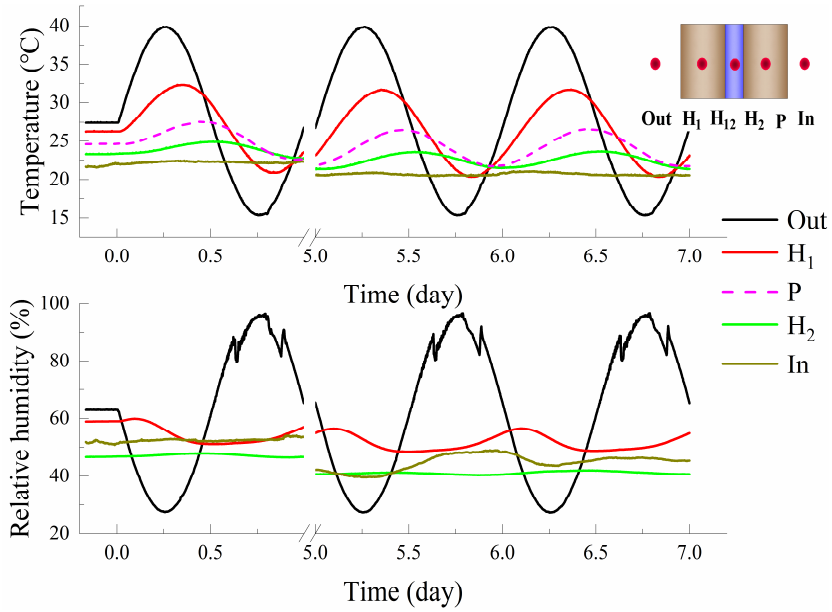

Fig. 6. Hygrothermal behavior of the configuration X = 0.5 L

3.2.3. PCM placed on the indoor side (X = 1 L)

The T/RH behavior of configuration X = 1 L is shown in Fig. 7, with only heat transfer and no moisture transfer occurred on the indoor side. The T amplitudes at H_1 and H_{12} were slightly smaller (0.1–0.2 °C) than in the configuration without PCM. Since there was little heat transfer between the indoor environment and the PCM, the PCM thermal inertia had little effect on the T distribution at H_1 and H_{12}. Inversely, the amplitude at H_2 was 0.1 °C higher than in the configuration without PCM,

which was caused by the thermal accumulation at H_2. Although there was little change in T amplitude compared to the configuration without PCM, time delays were still extended by 0.3, 0.7, and 1.2 h at points H_1, H_{12}, and H_2.

Compared with configuration without PCM, the RH amplitude was lower at H_{12} (3.7%), and slightly higher at H_2 (2.1%) because the PCM's impermeability caused moisture to accumulate around H_2. Therefore, the configuration X = 1 L should be avoided in practice because the moisture transfer between the envelope and the indoor environment was completely blocked by the PCM. However, in this study, this configuration was considered for comparison and as a reference for T/RH and energy analysis.

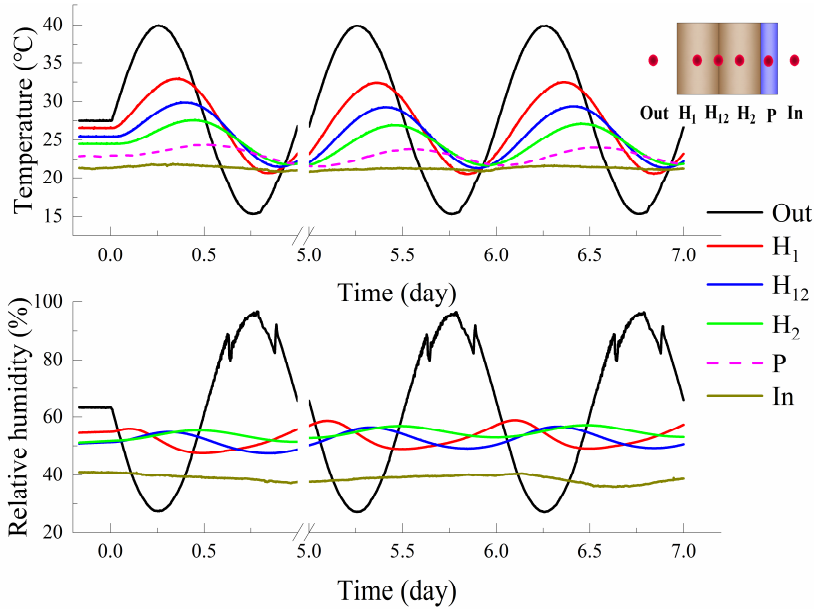

Fig. 7. Hygrothermal behavior of the configuration X = 1 L

315 **3.3. Summary of T/RH amplitudes and time delay**

316 Fig. 8(a) shows the mean daily T and RH amplitudes at H_1, H_{12}, and H_2 in the different
317 configurations. Due to the superposition effect at H_1, the magnitude order of RH and T amplitude at
318 different configurations was not consistent. However, for points H_{12} and H_2, higher T amplitudes
319 meant higher RH amplitudes.

320 To reduce indoor T/RH fluctuations, the T/RH amplitudes should ideally be low in the layer
321 closest to the indoor environment. Therefore, configuration X = 0.5 L was optimal, with the smallest T
322 and RH amplitudes (1.2 ℃ and 0.8%, respectively) at H_2, which were 50% and 60% less than in the
323 configuration without PCM (2.4 ℃ and 2.0%). Furthermore, compared with the outdoor T and RH
324 amplitudes, the reduction was as high as 90.4% and 97.7%, respectively, ensuring indoor hygrothermal
325 comfort under a wide range of outdoor T/RH fluctuations.

326

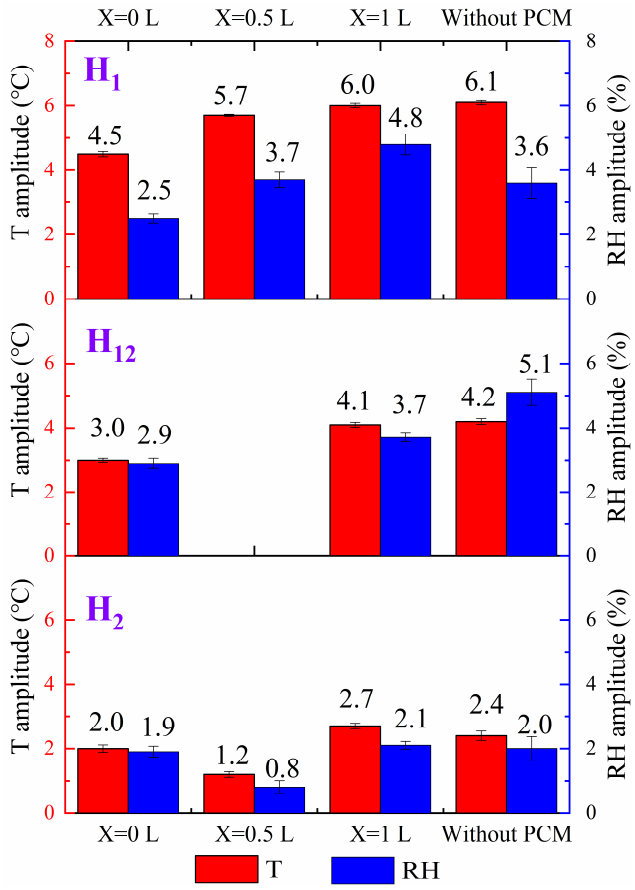

Fig. 8. T and RH amplitudes of hemp concrete in different configurations

Fig. 9 presents the relationship between the T amplitude and time delay. The time delay decreased almost linearly as the T amplitude increased from the outdoor side to the indoor side, reflecting the decay in T fluctuation over time. Both parameters were affected by the PCM, but the effect was different on the two sides of the PCM. Compared to the configuration without PCM, the T amplitude was reduced significantly at points between the PCM and the indoor side (H_1, H_{12}, and H_2 of configuration X = 0 L— reduced by 26.2%, 28.6%, and 16.7%; H_2 of configuration X = 0.5 L— reduced by as much as 50%). In contrast, for points between the PCM and the outdoor side (H_1 of configuration X = 0.5 L; H_1 and H_{12} of configuration X = 1 L), the reduction was less than 6.5%.

Similarly, the time delays at points between the PCM and the indoor side were extended by 56.8% to 114.3% compared to the configuration without PCM. But on the other side, the time delay was extended by less than 35%. Thus, the PCM had a significant effect on the T amplitude and time delay at points between the PCM and the indoor side, which explains the small T/RH amplitude at H_2 for the configuration X = 0.5 L.

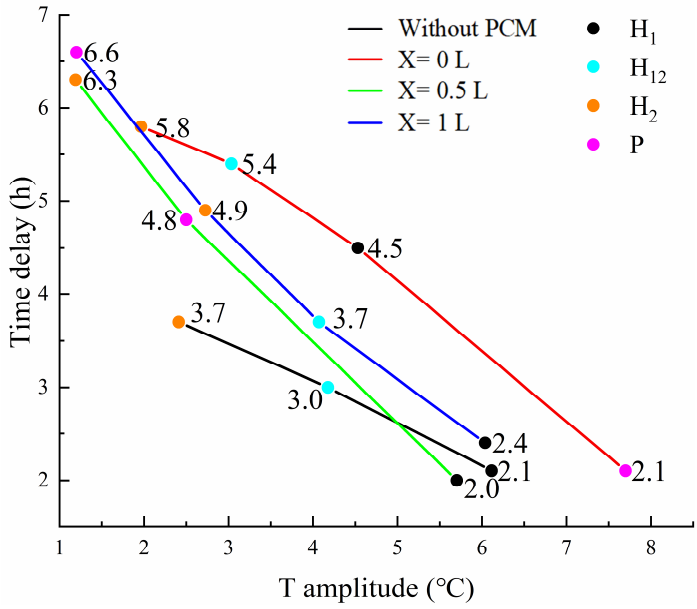

Fig. 9. T amplitude and time delay at different configurations and measurement points

It is worth noting that the closest layers to the indoor environment for configuration X = 1 L and X = 0.5 L (PCM layer and second concrete layer, respectively) had the smallest T amplitudes (1.2 °C for both) and almost the longest time delays (6.6 and 6.3 h, which were 78.4% and 70.3% longer than the configuration without PCM, respectively). In real buildings, these behaviors would have provided thermal comfort and shifted peak electricity demand. However, due to the moisture impermeability of the PCM positioned between the envelope and the indoor environment, the configuration X = 1 L

should be avoided. Therefore, configuration X = 0.5 L was considerable in terms of T/RH amplitude and time delay.

3.4. Heat flux and released/absorbed heat on the interior/exterior surface

Fig. 10(a) shows the heat flux on the interior and exterior surface of the envelope. On the interior surface, the configuration without PCM showed negative values for 6 h per day, indicating that the envelope released heat into the indoor environment for 18 h of the day. In comparison, the remaining configurations released heat for almost 24 h. For the heat flux amplitudes, the configuration without PCM was high because of the low thermal inertia. With the presence of PCM, the thermal inertia of the envelope was significantly improved, and the heat flux fluctuation was reduced. Configuration X = 0.5 L had the smallest amplitude at 4.4 W/m^2, which was 53.7%, 36.2%, and 36.2% less than configuration without PCM, X = 0 L, and X = 1 L.

As for the exterior surface, the heat flux fluctuation of configuration X = 0 L was the highest, indicating a great potential to absorb/release energy. Configurations X = 0.5 L and X = 1 L had similar fluctuations and were slightly higher than the configuration without PCM.

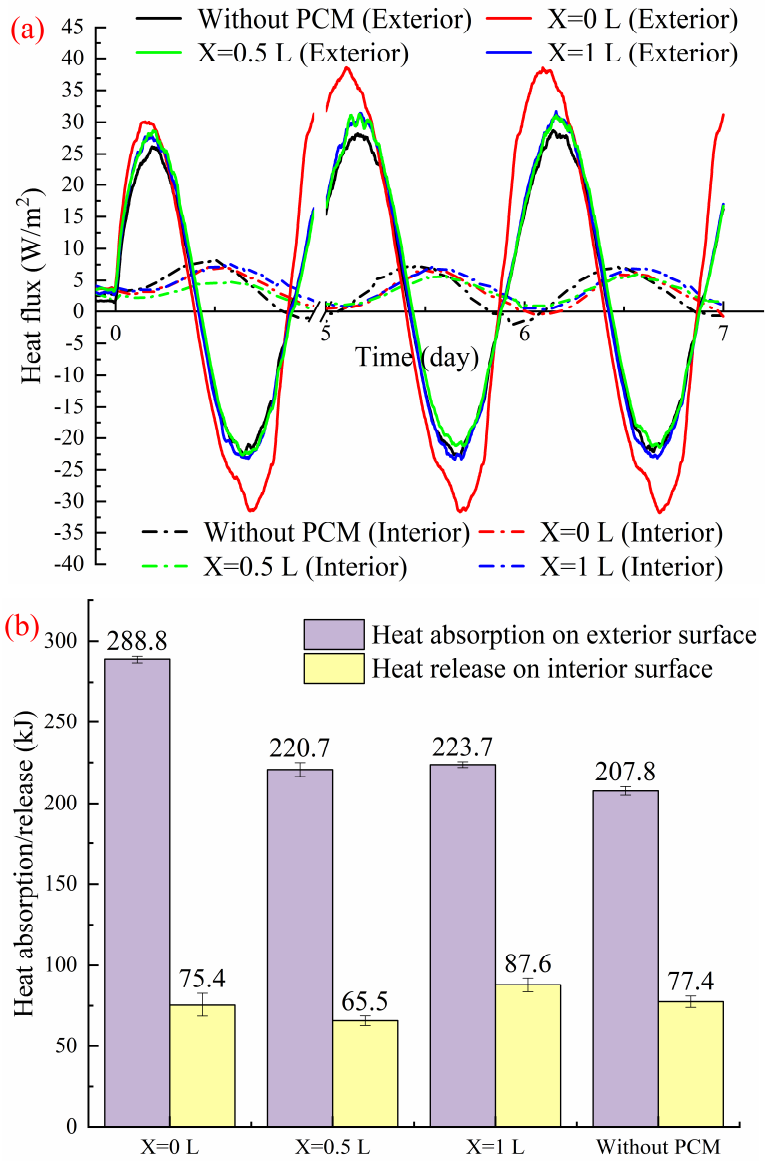

Fig. 10. (a) Heat flux on the exterior/interior surface; (b) Heat absorption/release on the exterior/interior surface

In order to calculate the released heat on the interior surface and the absorbed heat on the exterior, the calculation was implemented using the following formula:

$$Q = \int_{t_1}^{t_2} q\, A dt$$

where Q is the absorbed/released heat (J); t is time (s); t_1, t_2 are the start and the end time for the

calculation (s); q is the heat flux on both surfaces (W/m^2); and A is the transversal envelope area (m^2). It is noted that this formula can be applied to any material, whether the interior/exterior material is PCM or hemp concrete.

Fig. 10(b) summarizes the daily released heat on the interior surface and the absorbed heat on the exterior surface. The heat released on the interior surface represents a part of the building cooling load and affects the building's energy consumption. The released heat of the configuration without PCM was 77.4 kJ, which was higher than that of the configurations X = 0 L and X = 0.5 L. That is to say, the configuration without PCM released more heat in 18 h than the configurations X = 0 L and X = 0.5 L did in 24 h, which indirectly demonstrated the energy-saving potential of the PCM. For the configurations with PCM, their released heat changed in a non-linear manner as the PCM's location changed from the outdoor to the indoor side. Configuration X = 0.5 L released the least heat at 65.5 kJ, which was 13.1, 25.2, and 15.3% less than the configurations X = 0 L, X = 1 L, and without PCM, respectively. Therefore, the placement of the PCM in the middle of the envelope is promising based on its energy-saving potential.

As for the absorbed heat on the exterior surface, the heat of configuration X = 0 L (288.8 kJ) was significantly higher than those of the other configurations. The heat absorption of configurations X = 0.5 L and X = 1 L (220.7 and 223.7 kJ) was almost the same and slightly higher than the configuration without PCM (207.8 kJ). Therefore, the configuration with the PCM directly exposed to the outdoor environment adsorbed the most heat due to its higher thermal inertia, while the remaining three configurations with hemp concrete facing the outdoor environment adsorbed almost identical amounts of heat.

3.5 Energy storage/release by the whole envelope and the PCM

The heat flux difference on both sides of the envelope/PCM is plotted in Fig. 11(a). The configuration X = 0 L has the highest fluctuations for both the envelope and the PCM, indicating a high energy storage/release potential. The daily energy storage/release by the envelope/PCM is plotted in Fig. 11(b). For the envelope, the energy storage/release was very similar for the configurations X = 0.5 L, X = 1 L, and without PCM, while the configuration X = 0 L had the highest value. For the PCM, the energy storage/release capacity decreased significantly as the PCM moved away from the outdoor side. This trend is consistent with the proportion of energy storage/release by the PCM (on the right axis), which showed a linear downward trend from configuration X = 0 L to X = 0.5 L to X = 1 L. Therefore, when PCM was placed closer to the outdoor side, it had a greater role in participating the thermal energy management in the envelope.

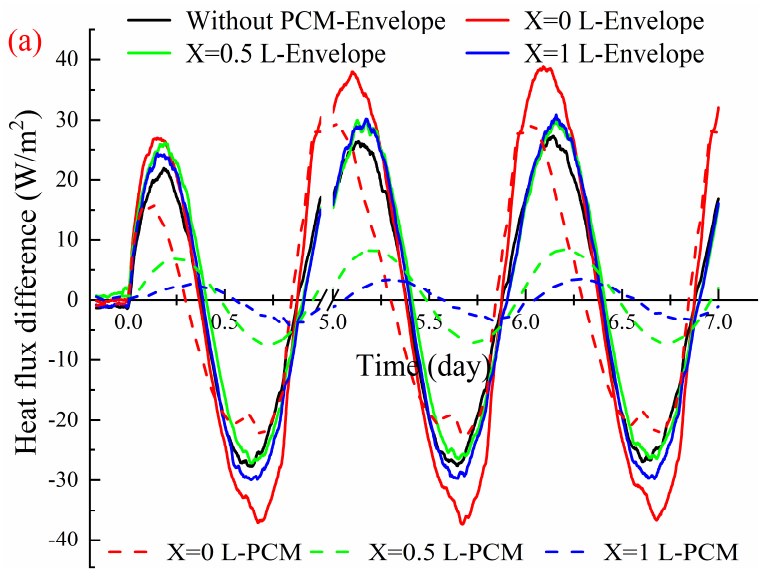

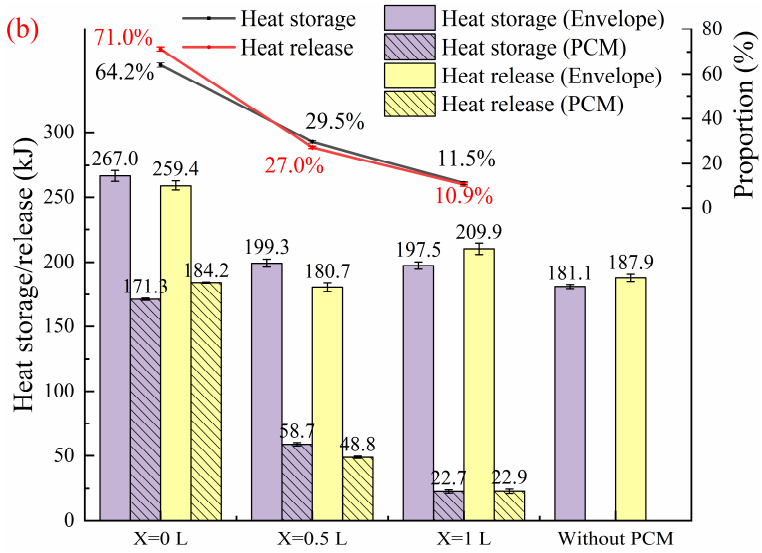

Fig. 11. (a) Heat flux difference of the envelope and the PCM; (b) Energy storage/release and the proportion of the PCM

As mentioned earlier, the absorbed heat on the exterior surface of the configuration X = 0 L was the highest, while the other three configurations were similar to each other (see Fig. 10(c)). The released heat on the exterior surface also followed this pattern (204.8, 140.4, 136.6, and 147.3 kJ for configurations X = 0 L, without PCM, X = 0.5 L, and X = 1 L, respectively). Therefore, when the PCM was placed on the outdoor side and interacted with the outdoor environment directly, the envelope and PCM tended to store/release more energy, and the energy participation of the PCM in the envelope was high. In contrast, when the PCM was far away from the outdoor side, the thermal interaction between the PCM and the outdoor environment was damped by one or two hemp concrete layers, which reduced the stored/released energy and the PCM's energy participation.

3.6 PCM activation and storage/release efficiency

This section discussed the PCM utilization, including its activation and energy efficiency. The melt fraction (f) represents the percentage of the activated (melted) PCM that has undergone the phase change. The PCM's storage/release efficiency (η) allows an assessment of how much latent heat has been utilized. The two equations for calculating the melt fraction and energy efficiency of PCM were expressed as:

$$f = \frac{T - T_s}{T_f - T_s}$$

$$\eta = \frac{E_{st}}{L} = \frac{\int_{t_s}^{t_f} \Delta q A dt}{\int_{T_s}^{T_f} m C_p dT}$$

where T is the mean T of the PCM (°C); T_s, T_f are the initial and final T of melting (°C); E_{st} is the actual latent thermal energy stored/released by the PCM (J/kg); L the PCM's total latent thermal energy (J/kg); t_f, t_s are the start and end time for the calculation (s); Δq is the heat flux difference between the inflow and outflow of the PCM (W/m^2); A the transversal envelope area (m^2); m is the mass of the PCM (kg); and C_p is the specific heat capacity of the PCM (J/(kg·K)).

The middle T of the PCM (point P) is considered the mean T of the PCM and is shown on the left axis of Fig. 12(a). On the right axis, the corresponding melt fraction is plotted. Since the phase change T ranges from 10 to 28 °C, the mean T of the configurations X = 0.5 and X = 1 L both lie within the phase change range. Their corresponding melt fractions were below 100% (80.1–97.7% and 64.8–69.2%, respectively), indicating that the PCM was partially melted and the configurations X = 0.5 L was more activated. Under the circumstances, phase change continued throughout the experiment period and energy was stored/released only in the latent heat mode. For the configuration

X = 0 L, the PCM's melt fraction was equal to 100% for almost half the day (11.5 h), implying that it remained in the liquid state and the energy storage/release was mainly taking place by the sensible heat mode during this period. For the remaining 12.5 h, with the melt fraction below 100%, the PCM was in a liquid-solid coexistence state and the energy storage/release was in latent heat mode.

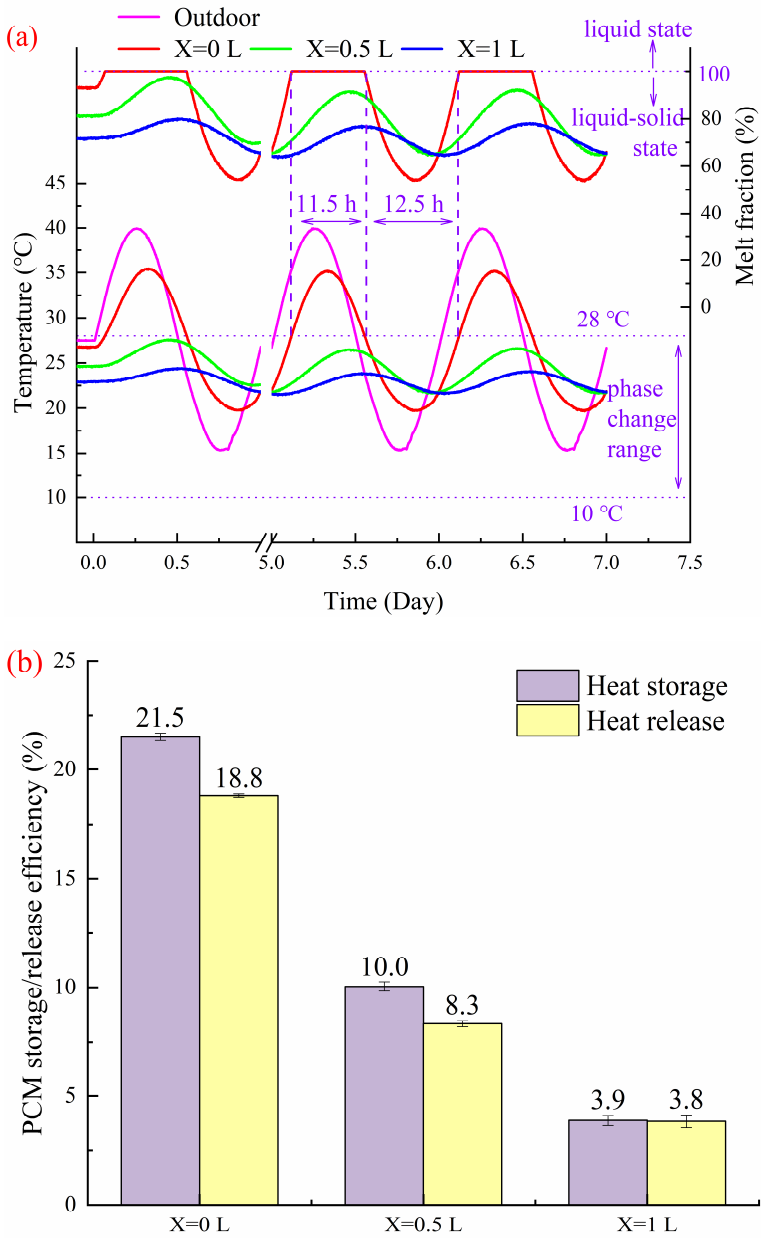

Fig. 12. (a) PCM's mean T and melt fraction; (b) PCM's storage/release efficiency

The PCM's daily storage/release efficiency is plotted in Fig. 12(b). It is notable that these values were significantly lower than the melt fraction due to the non-uniformity between the specific heat capacity and T. Furthermore, the PCM storage/release efficiency in this study was not high: the highest value was only 21.5%. This is because its value is affected by several factors, such as the convective heat transfer coefficient, boundary T, and peak melt T [53-56]. Since the experiment was done with the given boundary conditions, PCM, etc., the efficiency could not reach its optimal value. Nevertheless, this study concerns the relationship between the PCM's efficiency and its location in the envelope. For the values, the highest PCM storage/release efficiency was 21.5%/18.8%, which was 2.2/2.3 and 5.7/4.9 times higher than the configurations X = 0.5 L and 1 L, respectively. It should be remembered that the efficiency of configuration X=0 L was only generated for about half of the day (latent heat mode for 12.5 h, see Fig. 12(a)). Hence, when located close to the outdoor side, the PCM was more likely to be activated and had a higher efficiency.

However, although the PCM had a high efficiency when it was exposed to the outdoor environment directly (configuration X=0 L), it was liable to overactivation (overmelting, 11.5 h a day), which may increase the risk of leakage [57, 58]. The configuration X = 0.5 L is preferable because the PCM was kept in a partially melted state throughout the experimental period. Besides, the PCM's efficiency was more than twice as high as that of configuration X = 1 L for the same heat absorption on the exterior surface.

476 **3.7 Discussion**

477 Most of the prior studies related to PCM multilayer envelopes in the literature [35-41] focused on
478 thermal behavior and energy performance. However, the hygric behavior of the envelope was ignored
479 in these studies, even though porous materials (e.g., gypsum, plaster, wood, and concrete) that are part
480 of the PCM multilayer envelope have been proven to have hygroscopic properties [42-45]. In Sections
481 3.2 and 3.3, the RH amplitude was given special attention in addition to T amplitude and time delay.
482 The RH amplitudes at H_2 for configurations X=0 L and X=0.5 L were 1.9% and 0.8%, respectively,
483 both lower than the configuration without PCM of 2.0%. The configuration X=0.5 L absorbed/released
484 less heat from the outdoors (see Fig. 10) and the heat transfer to H_2 was damped by the PCM (high
485 melted but not overmelted, see Fig. 12), which was the reason for the smaller T/RH amplitude at H_2
486 than the configuration X=0 L. Therefore, both configurations, especially the configuration X=0.5 L,
487 were indicated to ensure not only low indoor T amplitude, low energy consumption, and long peak T
488 delay, as mentioned in [35-41], but also the low indoor RH amplitude as proved in this study.

489 In addition, in previous experimental studies related to the hygrothermal behavior of the
490 hygroscopic materials, static or static-to-static boundary conditions [17-20] were often implemented,
491 and dynamic boundary conditions [21] were rarely used. In the study [21] using sinusoidal boundary
492 conditions, the T and RH amplitudes in the middle of hemp concrete were reduced by 63% and 80%,
493 respectively, compared to the outdoors. In this paper, the reductions were further increased with the
494 addition of PCM. The T and RH amplitude reductions at the corresponding location (point H_{12}) for the
495 configuration X = 0 L were 76% and 92%, respectively, compared to the outdoors (see Fig. 5 and Fig.
496 8). The results were satisfactory as expected because of the damping effect of the PCM on outdoor heat

497 and the leading role of T on RH.

498 Furthermore, when evaluating the optimal PCM location for the PCM multilayer envelope,
499 thermal behavior [35, 41] and energy performance [36, 38-40] were often used as evaluation metrics in
500 prior studies. However, the findings of this paper recommended that the hygric properties of the
501 envelope also need to be considered. Also, the T behavior should be the main focus because of the
502 variation/amplitude consistency of T and RH at H_2 (see Fig. 8). On the other hand, determining the
503 optimal PCM location is complex because it also depends on the thermal properties of the PCM
504 (thickness, latent heat, phase transition interval, etc.) and the boundary environmental conditions [58],
505 in addition to the evaluation metrics. This is the reason that the optimal PCM location varies in
506 different literature [35-41]. However, this study focused more on the interaction between PCM and
507 hygroscopic material and the effect of PCM and its location on the hygric behavior of the hygroscopic
508 material. Therefore, a further recommendation can be applied to any type of PCM multilayer envelope
509 integrated by a PCM and a hygroscopic material. The reduction of T and RH amplitudes can be
510 achieved simultaneously by optimizing the location or thermal properties of the PCM.

511

512 ## 4. Conclusion

513 In this study, PCM and hemp concrete were integrated into a novel multilayer building envelope
514 that enables simultaneous T/RH regulation and energy savings. Three configurations with PCM placed
515 in different locations were experimentally compared with a configuration without PCM to study the
516 effect of PCM and its location on the hygrothermal behavior and energy performance of the envelope.

The primary conclusions and recommendations can be drawn as follows:

T plays a dominant role in affecting the RH variation at locations close to the indoor side. Since the moisture-buffering capacity of hemp concrete increases as T decreases, the presence of the PCM damped the T fluctuation, which increased the moisture retention capacity and reduced the RH fluctuation of the hemp concrete. Besides, the PCM's location affected the hygrothermal behavior and energy performance of the integrated envelope.

When the PCM was placed on the outdoor side, it had the highest energy participation (64.2%/71.0%) and storage/release efficiency (21.5%/18.8%) during the energy storage/release process. However, the PCM absorbed more heat from the outdoors than in other configurations, causing the overmelting of the PCM (11.5 h) and the high T/RH amplitude of the envelope.

PCM placed on the indoor side improved the thermal behavior of the envelope as it resulted in the smallest T fluctuation and the longest peak T delay at locations close to the indoor side. However, the PCM hindered the hemp concrete's ability to regulate the indoor RH.

The placement of the PCM in the middle of the envelope was recommended. The PCM was kept in a partially melted state with a high melt fraction of 80.1–97.7%, which resulted in the smallest indoor T/RH amplitude and the greatest energy savings. Compared to the configuration without PCM, the T/RH amplitude was reduced by 50%/60% and the peak T was delayed by 70.3% at locations close to the indoor side. Also, the energy consumption was reduced by 15.3%.

The current work is a start, and future study aims to explore the performance of the integrated envelope with PCM placed at more locations under different climates by numerical approach.

CRediT authorship contribution statement

Dongxia Wu: Conceptualization, Methodology, Investigation, Data curation, Formal analysis, Writing - original draft. **Mourad Rahim:** Conceptualization, Methodology, Investigation, Formal analysis, Writing - review & editing. **Mohammed El Ganaoui:** Supervision, Project administration, Conceptualization, Methodology, Formal analysis, Writing - review & editing. **Rachid Bennacer:** Conceptualization, Methodology, Formal analysis, Writing - review & editing. **Rabah Djedjig:** Methodology, Review & editing**. Bin Liu:** Methodology, Review & editing

Acknowledgements

We thank to the China Scholarship Council (CSC) for its financial support to the first author, No. 201808120084. CPER UL/Lorraine Region, PHC Maghreb, and EMPP Scientific Pole of the University of Lorraine are also acknowledged.

Funding

This research did not receive any specific grant from funding agencies in the public, commercial, or not-for-profit sectors.

References

[1] IEA, World Energy Outlook 2019, 2019.
https://www.nordicenergy.org/wp-content/uploads/2019/12/6.2_12-Dec_14.00-14.30_WEOslides-for-DT-for-COP25-FI

NAL.pdf. (accessed 04 December 2021).
[2] I.E.A. (IEA), Towards a zero-emission, efficient, and resilient buildings and construction sector, 2018. https://www.worldgbc.org/sites/default/files/2018%20GlobalABC%20Global%20Status%20Report.pdf. (accessed 01 July 2021).
[3] J. Fernandes, R. Mateus, H. Gervásio, S.M. Silva, L. Bragança, Passive strategies used in Southern Portugal vernacular rammed earth buildings and their influence in thermal performance, Renewable Energy 142 (2019) 345-363.https://doi.org/10.1016/j.renene.2019.04.098
[4] ASHRAE, Thermal environmental conditions for human occupancy, American Society of Heating, Refrigerating and Air-Conditioning Engineers, 2013
[5] C. Zuo, L. Luo, W. Liu, Effects of increased humidity on physiological responses, thermal comfort, perceived air quality, and Sick Building Syndrome symptoms at elevated indoor temperatures for subjects in a hot-humid climate, Indoor Air 31(2) (2021) 524-540.https://doi.org/10.1111/ina.12739
[6] B. Jones, C. Molina, Indoor Air Quality, in: M.A. Abraham (Ed.), Encyclopedia of Sustainable Technologies, Elsevier, Oxford, 2017, pp. 197-207.https://doi.org/10.1016/B978-0-12-409548-9.10198-8
[7] H.J. Moon, S.H. Ryu, J.T. Kim, The effect of moisture transportation on energy efficiency and IAQ in residential buildings, Energy and Buildings 75 (2014) 439-446.https://doi.org/10.1016/j.enbuild.2014.02.039
[8] B. Agoudjil, A. Benchabane, A. Boudenne, L. Ibos, M. Fois, Renewable materials to reduce building heat loss: Characterization of date palm wood, Energy and Buildings 43(2) (2011) 491-497.https://doi.org/10.1016/j.enbuild.2010.10.014
[9] F. Asdrubali, F. D'Alessandro, S. Schiavoni, A review of unconventional sustainable building insulation materials, Sustainable Materials and Technologies 4 (2015) 1-17.https://doi.org/10.1016/j.susmat.2015.05.002
[10] L. Gustavsson, A. Joelsson, R. Sathre, Life cycle primary energy use and carbon emission of an eight-storey wood-framed apartment building, Energy and Buildings 42(2) (2010) 230-242.https://doi.org/10.1016/j.enbuild.2009.08.018
[11] T. Jami, S.R. Karade, L.P. Singh, A review of the properties of hemp concrete for green building applications, Journal of Cleaner Production 239 (2019) 117852.https://doi.org/10.1016/j.jclepro.2019.117852
[12] L. Liu, H. Li, A. Lazzaretto, G. Manente, C. Tong, Q. Liu, N. Li, The development history and prospects of biomass-based insulation materials for buildings, Renewable and Sustainable Energy Reviews 69 (2017) 912-932.https://doi.org/10.1016/j.rser.2016.11.140
[13] B. Time, Hygroscopic moisture transport in wood, PhD thesis, Norwegian University of Science and Technology Trondheim, 1998
[14] R. Shmulsky, P.D. Jones, Forest products and wood science: an introduction, John Wiley & Sons2019
[15] R.M. Barbosa, N. Mendes, Combined simulation of central HVAC systems with a whole-building hygrothermal model, Energy and Buildings 40(3) (2008) 276-288.https://doi.org/10.1016/j.enbuild.2007.02.022
[16] O.F. Osanyintola, C.J. Simonson, Moisture buffering capacity of hygroscopic building materials: Experimental facilities and energy impact, Energy and Buildings 38(10) (2006) 1270-1282.https://doi.org/10.1016/j.enbuild.2006.03.026
[17] T. Colinart, P. Glouannec, T. Pierre, P. Chauvelon, A. Magueresse, Experimental Study on the Hygrothermal Behavior of a Coated Sprayed Hemp Concrete Wall, Buildings 3(1) (2013).https://doi.org/10.3390/buildings3010079
[18] N. Chennouf, B. Agoudjil, T. Alioua, A. Boudenne, K. Benzarti, Experimental investigation on hygrothermal performance of a bio-based wall made of cement mortar filled with date palm fibers, Energy and Buildings 202 (2019)

109413.https://doi.org/10.1016/j.enbuild.2019.109413
[19] Y. Aït Oumeziane, S. Moissette, M. Bart, F. Collet, S. Pretot, C. Lanos, Influence of hysteresis on the transient hygrothermal response of a hemp concrete wall, Journal of Building Performance Simulation 10(3) (2017) 256-271.https://doi.org/10.1080/19401493.2016.1216166
[20] F. Collet, S. Pretot, Experimental highlight of hygrothermal phenomena in hemp concrete wall, Building and Environment 82 (2014) 459-466.https://doi.org/10.1016/j.buildenv.2014.09.018
[21] M. Rahim, O. Douzane, A.D. Tran Le, G. Promis, T. Langlet, Experimental investigation of hygrothermal behavior of two bio-based building envelopes, Energy and Buildings 139 (2017) 608-615.https://doi.org/10.1016/j.enbuild.2017.01.058
[22] S. Poyet, S. Charles, Temperature dependence of the sorption isotherms of cement-based materials: Heat of sorption and Clausius–Clapeyron formula, Cement and Concrete Research 39(11) (2009) 1060-1067.https://doi.org/10.1016/j.cemconres.2009.07.018
[23] T. Colinart, P. Glouannec, Temperature dependence of sorption isotherm of hygroscopic building materials. Part 1: Experimental evidence and modeling, Energy and Buildings 139 (2017) 360-370.https://doi.org/10.1016/j.enbuild.2016.12.082
[24] T. Colinart, P. Glouannec, M. Bendouma, P. Chauvelon, Temperature dependence of sorption isotherm of hygroscopic building materials. Part 2: Influence on hygrothermal behavior of hemp concrete, Energy and Buildings 152 (2017) 42-51.https://doi.org/10.1016/j.enbuild.2017.07.016
[25] R. Saxena, D. Rakshit, S.C. Kaushik, Experimental assessment of Phase Change Material (PCM) embedded bricks for passive conditioning in buildings, Renewable Energy 149 (2020) 587-599.https://doi.org/10.1016/j.renene.2019.12.081
[26] L. Yang, J.-n. Huang, F. Zhou, Thermophysical properties and applications of nano-enhanced PCMs: An update review, Energy Conversion and Management 214 (2020) 112876.https://doi.org/10.1016/j.enconman.2020.112876
[27] M. Ahangari, M. Maerefat, An innovative PCM system for thermal comfort improvement and energy demand reduction in building under different climate conditions, Sustainable Cities and Society 44 (2019) 120-129.https://doi.org/10.1016/j.scs.2018.09.008
[28] P.K.S. Rathore, S.K. Shukla, Potential of macroencapsulated PCM for thermal energy storage in buildings: A comprehensive review, Construction and Building Materials 225 (2019) 723-744.https://doi.org/10.1016/j.conbuildmat.2019.07.221
[29] A. Fateh, D. Borelli, H. Weinläder, F. Devia, Cardinal orientation and melting temperature effects for PCM-enhanced light-walls in different climates, Sustainable Cities and Society 51 (2019) 101766.https://doi.org/10.1016/j.scs.2019.101766
[30] S.H. Choi, J. Park, H.S. Ko, S.W. Karng, Heat penetration reduction through PCM walls via bubble injections in buildings, Energy Conversion and Management 221 (2020) 113187.https://doi.org/10.1016/j.enconman.2020.113187
[31] S. Serrano, C. Barreneche, A. Navarro, L. Haurie, A.I. Fernandez, L.F. Cabeza, Use of multi-layered PCM gypsums to improve fire response. Physical, thermal and mechanical characterization, Energy and Buildings 127 (2016) 1-9.https://doi.org/10.1016/j.enbuild.2016.05.056
[32] A. Mechouet, E.M. Oualim, T. Mouhib, Effect of mechanical ventilation on the improvement of the thermal performance of PCM-incorporated double external walls: A numerical investigation under different climatic conditions in Morocco, Journal of Energy Storage 38 (2021) 102495.https://doi.org/10.1016/j.est.2021.102495
[33] S.J. Chang, Y. Kang, S. Wi, S.-G. Jeong, S. Kim, Hygrothermal performance improvement of the Korean wood

640 frame walls using macro-packed phase change materials (MPPCM), Applied Thermal Engineering 114 (2017)
641 457-465.https://doi.org/10.1016/j.applthermaleng.2016.11.188
642 [34] N. Essid, A. Eddhahak, J. Neji, Experimental and numerical analysis of the energy efficiency of PCM concrete
643 wallboards under different thermal scenarios, Journal of Building Engineering 45 (2022)
644 103547.https://doi.org/10.1016/j.jobe.2021.103547
645 [35] K.O. Lee, M.A. Medina, E. Raith, X. Sun, Assessing the integration of a thin phase change material (PCM) layer in
646 a residential building wall for heat transfer reduction and management, Applied Energy 137 (2015)
647 699-706.https://doi.org/10.1016/j.apenergy.2014.09.003
648 [36] A. Fateh, F. Klinker, M. Brütting, H. Weinläder, F. Devia, Numerical and experimental investigation of an insulation
649 layer with phase change materials (PCMs), Energy and Buildings 153 (2017)
650 231-240.https://doi.org/10.1016/j.enbuild.2017.08.007
651 [37] A. Fateh, D. Borelli, F. Devia, H. Weinläder, Summer thermal performances of PCM-integrated insulation layers for
652 light-weight building walls: Effect of orientation and melting point temperature, Thermal Science and Engineering
653 Progress 6 (2018) 361-369.https://doi.org/10.1016/j.tsep.2017.12.012
654 [38] R.A. Kishore, M.V.A. Bianchi, C. Booten, J. Vidal, R. Jackson, Optimizing PCM-integrated walls for potential
655 energy savings in U.S. Buildings, Energy and Buildings 226 (2020)
656 110355.https://doi.org/10.1016/j.enbuild.2020.110355
657 [39] R.A. Kishore, M.V.A. Bianchi, C. Booten, J. Vidal, R. Jackson, Parametric and sensitivity analysis of a
658 PCM-integrated wall for optimal thermal load modulation in lightweight buildings, Applied Thermal Engineering 187
659 (2021) 116568.https://doi.org/10.1016/j.applthermaleng.2021.116568
660 [40] E. Köse Murathan, G. Manioğlu, Evaluation of phase change materials used in building components for
661 conservation of energy in buildings in hot dry climatic regions, Renewable Energy 162 (2020)
662 1919-1930.https://doi.org/10.1016/j.renene.2020.09.086
663 [41] Z.X. Li, A.A.A.A. Al-Rashed, M. Rostamzadeh, R. Kalbasi, A. Shahsavar, M. Afrand, Heat transfer reduction in
664 buildings by embedding phase change material in multi-layer walls: Effects of repositioning, thermophysical properties
665 and thickness of PCM, Energy Conversion and Management 195 (2019)
666 43-56.https://doi.org/10.1016/j.enconman.2019.04.075
667 [42] H. Zhang, C. Shi, D. Pan, Y. Xuan, X. He, Optimization of effective moisture penetration depth model considering
668 airflow velocity for gypsum-based materials, Journal of Building Engineering 32 (2020)
669 101539.https://doi.org/10.1016/j.jobe.2020.101539
670 [43] T. Santos, M.I. Gomes, A.S. Silva, E. Ferraz, P. Faria, Comparison of mineralogical, mechanical and hygroscopic
671 characteristic of earthen, gypsum and cement-based plasters, Construction and Building Materials 254 (2020)
672 119222.https://doi.org/10.1016/j.conbuildmat.2020.119222
673 [44] M. Asli, F. Brachelet, E. Sassine, E. Antczak, Thermal and hygroscopic study of hemp concrete in real ambient
674 conditions, Journal of Building Engineering 44 (2021) 102612.https://doi.org/10.1016/j.jobe.2021.102612
675 [45] M. Rahim, R. Djedjig, D. Wu, R. Bennacer, M.E.L. Ganaoui, Experimental investigation of hygrothermal behavior
676 of wooden-frame house under real climate conditions, Energy and Built Environment
677 (2021).https://doi.org/10.1016/j.enbenv.2021.09.002
678 [46] M. Rahim, O. Douzane, A.D. Tran Le, G. Promis, B. Laidoudi, A. Crigny, B. Dupre, T. Langlet, Characterization of
679 flax lime and hemp lime concretes: Hygric properties and moisture buffer capacity, Energy and Buildings 88 (2015)
680 91-99.https://doi.org/10.1016/j.enbuild.2014.11.043

[47] D. Energain®, Hydrocarbon-based PCM Applications, 2010. https://cdn2.hubspot.net/hub/55819/file-14755587-pdf/docs/buildings-xi/dupont_energain.pdf. (accessed 04 December 2021).
[48] M. Rahim, A.D. Tran Le, O. Douzane, G. Promis, T. Langlet, Numerical investigation of the effect of non-isotherme sorption characteristics on hygrothermal behavior of two bio-based building walls, Journal of Building Engineering 7 (2016) 263-272.https://doi.org/10.1016/j.jobe.2016.07.003
[49] G. Costantine, C. Maalouf, T. Moussa, G. Polidori, Experimental and numerical investigations of thermal performance of a Hemp Lime external building insulation, Building and Environment 131 (2018) 140-153.https://doi.org/10.1016/j.buildenv.2017.12.037
[50] A.D. Tran Le, C. Maalouf, T.H. Mai, E. Wurtz, F. Collet, Transient hygrothermal behaviour of a hemp concrete building envelope, Energy and Buildings 42(10) (2010) 1797-1806.https://doi.org/10.1016/j.enbuild.2010.05.016
[51] Y. Liu, Y. Wang, D. Wang, J. Liu, Effect of moisture transfer on internal surface temperature, Energy and Buildings 60 (2013) 83-91.https://doi.org/10.1016/j.enbuild.2013.01.019
[52] H. Djamila, Indoor thermal comfort predictions: Selected issues and trends, Renewable and Sustainable Energy Reviews 74 (2017) 569-580.https://doi.org/10.1016/j.rser.2017.02.076
[53] I. Adilkhanova, S.A. Memon, J. Kim, A. Sheriyev, A novel approach to investigate the thermal comfort of the lightweight relocatable building integrated with PCM in different climates of Kazakhstan during summertime, Energy 217 (2021) 119390.https://doi.org/10.1016/j.energy.2020.119390
[54] G. Evola, L. Marletta, F. Sicurella, A methodology for investigating the effectiveness of PCM wallboards for summer thermal comfort in buildings, Building and Environment 59 (2013) 517-527.https://doi.org/10.1016/j.buildenv.2012.09.021
[55] D.A. Neeper, Thermal dynamics of wallboard with latent heat storage, Solar Energy 68(5) (2000) 393-403.https://doi.org/10.1016/S0038-092X(00)00012-8
[56] K. Peippo, P. Kauranen, P.D. Lund, A multicomponent PCM wall optimized for passive solar heating, Energy and Buildings 17(4) (1991) 259-270.https://doi.org/10.1016/0378-7788(91)90009-R
[57] P.K.S. Rathore, S.K. Shukla, Enhanced thermophysical properties of organic PCM through shape stabilization for thermal energy storage in buildings: A state of the art review, Energy and Buildings 236 (2021) 110799.https://doi.org/10.1016/j.enbuild.2021.110799
[58] S. Drissi, T.-C. Ling, K.H. Mo, Thermal performance of a solar energy storage concrete panel incorporating phase change material aggregates developed for thermal regulation in buildings, Renewable Energy 160 (2020) 817-829.https://doi.org/10.1016/j.renene.2020.06.076